per nucleus (*16*) even though oxygen ions have not yet been detected by the LECP or the plasma science experiments (*13*). This may mean that oxygen ions are not efficiently accelerated to energies (≳0.6 MeV per nucleon) at which composition data are available or that oxygen ions are preferentially lost.

The Uranian magnetosphere may be characterized by an efficient mechanism for preferentially removing energetic ions, as opposed to electrons, from the radiation belts, even though loss rates due to sweeping by satellites are comparable for ions and electrons at energies observed by the LECP instrument. One candidate mechanism is charge exchange in an extended hydrogen atmosphere if one is present (*14*); another is wave-particle interactions. Preferential ion loss is supported by the observation that the energetic ion β is substantially less than that found at Saturn, whereas the electron β is comparable to Saturnian values. The total plasma β is then much less than 1, so that particle stresses do not greatly distort the field at Uranus. Since large day-night asymmetries are observed in the radiation belts outside the orbit of Umbriel, there may be a significantly nondipolar magnetic field at these distances in which magnetopause currents take an important part.

REFERENCES AND NOTES

1. L. J. Lanzerotti and S. M. Krimigis, *Phys. Today* **38**, 25 (1985).
2. N. F. Ness *et al.*, *Science* **233**, 85 (1986).
3. J. W. Warwick *et al.*, *ibid.*, p. 102.
4. S. M. Krimigis *et al.*, *Space Sci. Rev.* **21**, 329 (1977).
5. S. M. Krimigis *et al.*, *Science* **204**, 998 (1979).
6. Because of damage to the thinnest (2-μm) LECP detector during the Voyager 2 encounter with Saturn's magnetosphere, the lowest energy ion species separated in Uranus' magnetosphere (≳0.6 MeV per nucleon) was higher than that separated during the encounter with Jupiter and Saturn (≳0.2 MeV per nucleon).
7. D. C. Hamilton, D. C. Brown, G. Gloeckler, W. I. Axford, *J. Geophys. Res.* **88**, 8905 (1983).
8. J. F. Carbary and S. M. Krimigis, *Geophys. Res. Lett.* **9**, 1073 (1982).
9. S. M. Krimigis, R. D. Zwickl, D. N. Baker, *J. Geophys. Res.* **90**, 3947 (1985).
10. S. M. Krimigis, in *Proceedings of the Conference on Comparative Study of Magnetospheric Systems* (Centre National d'Etudes Spatiales, Toulouse, France, 1986), pp. 99–124.
11. G. Anagnostopoulos, E. T. Sarris, S. M. Krimigis, *J. Geophys. Res.* **91**, 3020 (1986).
12. S. M. Krimigis *et al.*, *ibid.* **88**, 8871 (1983).
13. H. S. Bridge *et al.*, *Science* **233**, 89 (1986).
14. A. L. Broadfoot *et al.*, *ibid.*, p. 74.
15. A. F. Cheng and L. J. Lanzerotti, *J. Geophys. Res.* **83**, 2597 (1978); L. J. Lanzerotti, W. L. Brown, K. J. Marcantonio, in preparation; L. Calcagno, L. G. Foti, L. Torrisi, G. Strazzullo, *Icarus* **63**, 31 (1985).
16. A. F. Cheng, in *Uranus and Neptune*, J. T. Bergstrahl, Ed. (*NASA Conf. Publ. 2330*, 1984), p. 541; ——— and T. W. Hill, *ibid.*, p. 557.
17. T. W. Hill, *ibid.*, p. 497; G. L. Siscoe, *Icarus* **24**, 311 (1975).

18. We thank the members of the Voyager project and personnel at the Jet Propulsion Laboratory and the Planetary Programs Office, NASA Headquarters, for help and cooperation in carrying out this experiment. We thank J. Carbary, M. Paonessa, B. J. Hook, L. Pacini, J. G. Gunther, D. C. Brown, C. G. Maclennan, and E. V. Bell, II for their enthusiasm and long hours in support of the project. The work of O. Divers (among many others) was essential to the success of our investigation. We thank the Voyager MAG team for making their field model available before publication. Supported by NASA under task I of contract N00024-85-C-5301 and by subcontract at the universities of Kansas and Maryland.

31 March 1986; accepted 5 May 1986

Voyager 2 Radio Observations of Uranus

JAMES W. WARWICK, DAVID R. EVANS, JOSEPH H. ROMIG, CONSTANCE B. SAWYER, MICHAEL D. DESCH, MICHAEL L. KAISER, JOSEPH K. ALEXANDER, THOMAS D. CARR, DAVID H. STAELIN, SAMUEL GULKIS, ROBERT L. POYNTER, MONIQUE AUBIER, ANDRE BOISCHOT, YOLANDE LEBLANC, ALAIN LECACHEUX, BENT M. PEDERSEN, PHILIPPE ZARKA

Within distances to Uranus of about 6 × 10^6 kilometers (inbound) and 35 × 10^6 kilometers (outbound), the planetary radio astronomy experiment aboard Voyager 2 detected a wide variety of radio emissions. The emission was modulated in a period of 17.24 ± 0.01 hours, which is identified as the rotation period of Uranus' magnetic field. Of the two poles where the axis of the off-center magnetic dipole (measured by the magnetometer experiment aboard Voyager 2) meets the planetary surface, the one closer to dipole center is now located on the nightside of the planet. The radio emission generally had maximum power and bandwidth when this pole was tipped toward the spacecraft. When the spacecraft entered the nightside hemisphere, which contains the stronger surface magnetic pole, the bandwidth increased dramatically and thereafter remained large. Dynamically evolving radio events of various kinds embedded in these emissions suggest a Uranian magnetosphere rich in magnetohydrodynamic phenomena.

RADIO EMISSIONS FROM URANUS were first detected through analysis of planetary radio astronomy (PRA) (*1*) data taken during the 5 days before Voyager 2's closest approach to the planet. In Fig. 1, a periodically varying signal is clearly present in the upper 58.8-kHz and upper 78.0-kHz channels as the spacecraft approached Uranus. The planetary signals, which were most intense in the upper channel, increased in amplitude as the spacecraft neared closest approach; strong spacecraft interference can be recognized by its shape as a function of time in both the upper and the lower channels for each frequency. No planetary signals occur at 39.6 kHz except near closest approach and, possibly, at DOY 19.2. This signal appears also at 58.8 kHz and in both upper and lower channels. Many similar, intense signals appear before closest approach at 58.8, 78.0, and 97.2 kHz, but we cannot identify with surety any of these as planetary signals. Emission was relatively weak in the 97.2-kHz channels until the spacecraft was near closest approach. The emission before encounter probably extended continuously from about 40 to 100 kHz.

Opposite states of circular polarization appear in upper and lower channels of the PRA instrument. The relation of upper or lower channel to polarization sense reversed near closest approach, when the direction to the source passed through the plane of the antenna. In the usual definition for radio science, the upper channel at each frequency is polarized in the left-hand sense before and in the right-hand sense after closest approach. Before closest approach, the emission was strongest in the upper channel for each frequency at which emission occurred; after closest approach, the emission was generally strongest in the lower channel for each frequency. With some important exceptions, the emissions were therefore left-hand polarized throughout encounter.

Figure 2 shows overview dynamic spectra covering the 4-day period near closest approach. The great increase and subsequent decrease in intensity is apparent at most frequencies, and there was an enormous extension in emission bandwidth to higher frequencies (up to 800 kHz) that began just before closest approach. This high-frequen-

J. W. Warwick, D. R. Evans, J. H. Romig, C. B. Sawyer, Radiophysics, Inc., Boulder, CO 80301.
M. D. Desch and M. L. Kaiser, Laboratory for Extraterrestrial Physics, Goddard Space Flight Center, Greenbelt, MD 20771.
J. K. Alexander, NASA Headquarters, Washington, DC, 20546.
T. D. Carr, Department of Astronomy, University of Florida, Gainesville, FL 32611.
D. H. Staelin, Research Laboratory of Electronics, Massachusetts Institute of Technology, Cambridge, MA 02319.
S. Gulkis and R. L. Poynter, Jet Propulsion Laboratory, California Institute of Technology, Pasadena, CA 91109.
M. Aubier, A. Boischot, Y. Leblanc, A. Lecacheux, B. M. Pedersen, P. Zarka, Observatoire de Paris, Section d'Astrophysique, 92190 Meudon, France.

cy emission continued throughout the outbound phase. Its characteristics, save for the greater intensity and bandwidth, are similar to the continuum radiation seen inbound.

Emissions from the outbound trajectory repeated often and consisted of a smoothly varying component that was followed by bursts. In cycles the smooth component increased in both bandwidth and intensity and then decreased almost beyond the limits of detection. At the time of maximum frequency (and maximum bandwidth), a sharp "bite" occurred in the smooth emissions above about 300 kHz. Examples of this bite appear at 17 hours spacecraft event time on 25 January and again at 10 hours on 26 January. During the interval when the smooth component was weakest (but not the bite itself), bursty emission was evident from 0 to 4 hours and from 17 to 23 hours on 26 January.

The fundamental morphology of the continuum after encounter is seen again in Fig. 3, which shows five consecutive rotations beginning at 12 hours spacecraft event time on 25 January (rotation refers to the value of a period, which will be discussed in more detail below). These records were taken at 481.2 kHz; their amplitudes were adjusted to represent a source at a constant distance from the spacecraft. During approximately 10 hours of each rotation only the smooth emission was observed; it was followed by bursty emission during the final 7 hours of the rotation. The bite feature occurred in the middle of the smooth emission at about 4.5 hours after the start of each cycle as presented in Fig. 3 and repeated every rotation.

Figure 4 shows the spectra for dayside and nightside Uranian emissions together with spectra for both Earth and Saturn. In comparing the various power levels, it should be recognized that Earth and Saturn emissions are characteristically very bursty, so that their power levels range over several orders of magnitude and are also often narrow band at any given instant. They are not considered continuums as are the Uranian emissions.

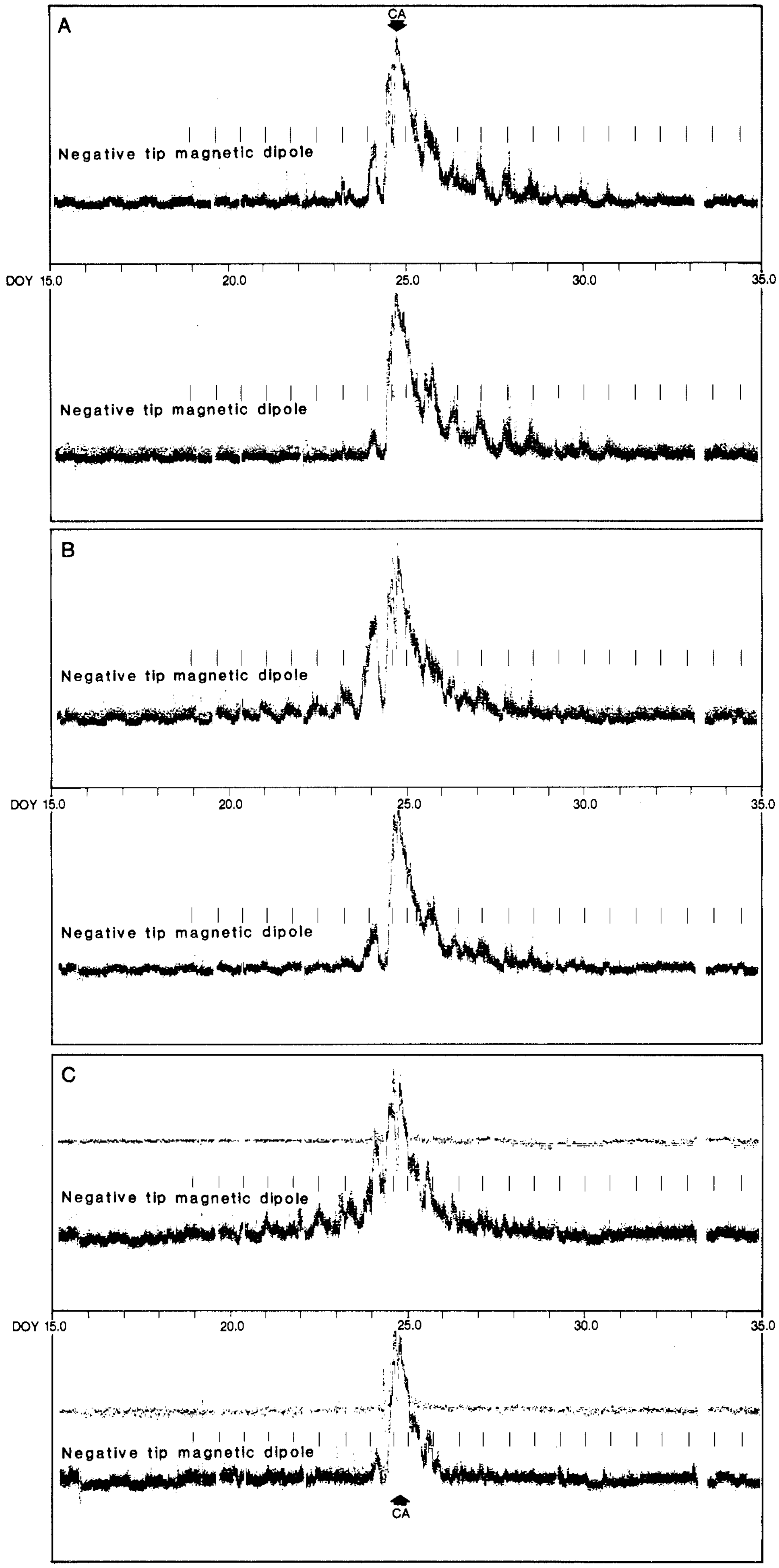

Fig. 1. Radio emissions from Uranus detected by Voyager 2's PRA experiment. An upper and a lower channel (with opposite circular polarization) are shown for 97.2 kHz (A), 78.0 kHz (B), and 58.8 kHz (C). The relation of polarization sense to channel reverses near closest approach (CA). Data number, which is approximately the logarithm of the signal levels (total range, 50 dB), is plotted as a function of time, day of the year (DOY). Before closest approach, the Uranian signals appear most strongly as a quasi-sinusoidal oscillation in the upper channels of 58.8 and 78.0 kHz; after closest approach, similar oscillations are strongest in the lower channel of 97.2 kHz. Short vertical lines mark times when the subspacecraft Uranus longitude is the same as that of the strong surface dipole tip.

On several occasions a periodic sequence of impulsive bursts appeared near 700 kHz, superposed on the main emissions (Fig. 5). Their repetition period was slightly more than 10 minutes. Examination of the dynamic spectra of these bursts shows them to be vertex-early arcs that cover a range of about 150 kHz. "Vertex-early" refers to the fact that these arcs are convex in shape, with the convexity directed toward earlier times. More than 15 successive bursts occurred in this instance. On a tiny scale in radio frequency and frequency range, these bursts resemble arcs in the spectrum of Jupiter's decametric radiation. There, either vertex-early or vertex-late arcs were the typical fine structure of the emission; they have been interpreted (*2*) in terms of bounce times of magnetohydrodynamic waves traveling along flux tubes in Jupiter's magnetosphere.

During the Uranian ring plane crossing at 4.57 Uranus radii (R_U), an additional signal was superposed on the smoothly varying continuum in the three low-frequency channels at 20.4, 39.6, and 58.8 kHz; the emission may have extended yet higher in frequency, although its spectrum was quite steep. The emission lasted about 2 minutes, which corresponds to spacecraft motion through about 1800 km perpendicular to the ring plane. We understand it as the response of the PRA receiver to the impact of minute ring particles on the spacecraft and the PRA antennas. A similar phenomenon occurred when Voyager 2's PRA antennas passed through the ring plane of Saturn (*3*).

A period slightly longer than 17 hours organizes the PRA data quite well over the entire encounter, including emissions before and after closest approach. After closest approach, similar features appeared repeatedly in the single-frequency plots (Fig. 3) and dynamic spectra (Fig. 2), which suggested that they might serve as time markers to define accurately the rotation period. The particular mark we chose was the bite, described above, which we recognized 19 times during 26 rotations of Uranus. The times of the bite in the 481.2-kHz channel were corrected for the motion in Uranian longitude of Voyager 2 on its outbound trajectory and their phases determined in terms of a 17.3-hour clock. There is a steady shift in the measured phases that yields the more accurate period of 17.24 ± 0.01 hours; the quoted error is the probable error of the least-squares straight-line fit to the phases. The bite represents an extremely good reference mark with highly predictable recurrence times. A similar situation holds for Jupiter's decametric emission, which has long been known to exhibit a permanent dynamic spectrum. The stability of the bite explains the unusually small uncertainty we derive for the period in spite of the relatively short time span of the data.

Uranus' low-frequency nonthermal emissions do not appear to depend strongly on local solar time and are similar in that respect to Jupiter's decametric emissions. Unlike that kind of emission from Jupiter, the Uranian emissions are probably generated at considerable distances above the planet's surface; before closest approach they were typically detected at heights of more than 1 R_U, if the emission frequency is the electron cyclotron frequency in the Uranian magnetic field (*4*). Only at the very highest frequencies after closest approach is the source of cyclotron emission close to the surface.

Figure 6 is a representation of the Uranian meridian plane containing the magnetic dipole. The left half-plane contains the spacecraft near those times before and after closest approach when we observed peak intensity radiation at frequencies below 300 kHz and at the center of the bite (Fig. 3) at higher frequencies. The dipole center is shifted about 0.3 R_U along the rotation axis into the rotational hemisphere away from the sun; its axis is tilted 60° to the rotational axis, which lies along the ordinate scale. Some dipole lines of force in this meridian place are identified by their L-shell values. The cuts of the specific dipole component surfaces on which 78.0- and 97.2-kHz radiation is hypothetically generated are shown as dashed lines.

Most planetary emissions depend strongly on latitude, and we anticipated similar dependence of the Uranus emission. We find,

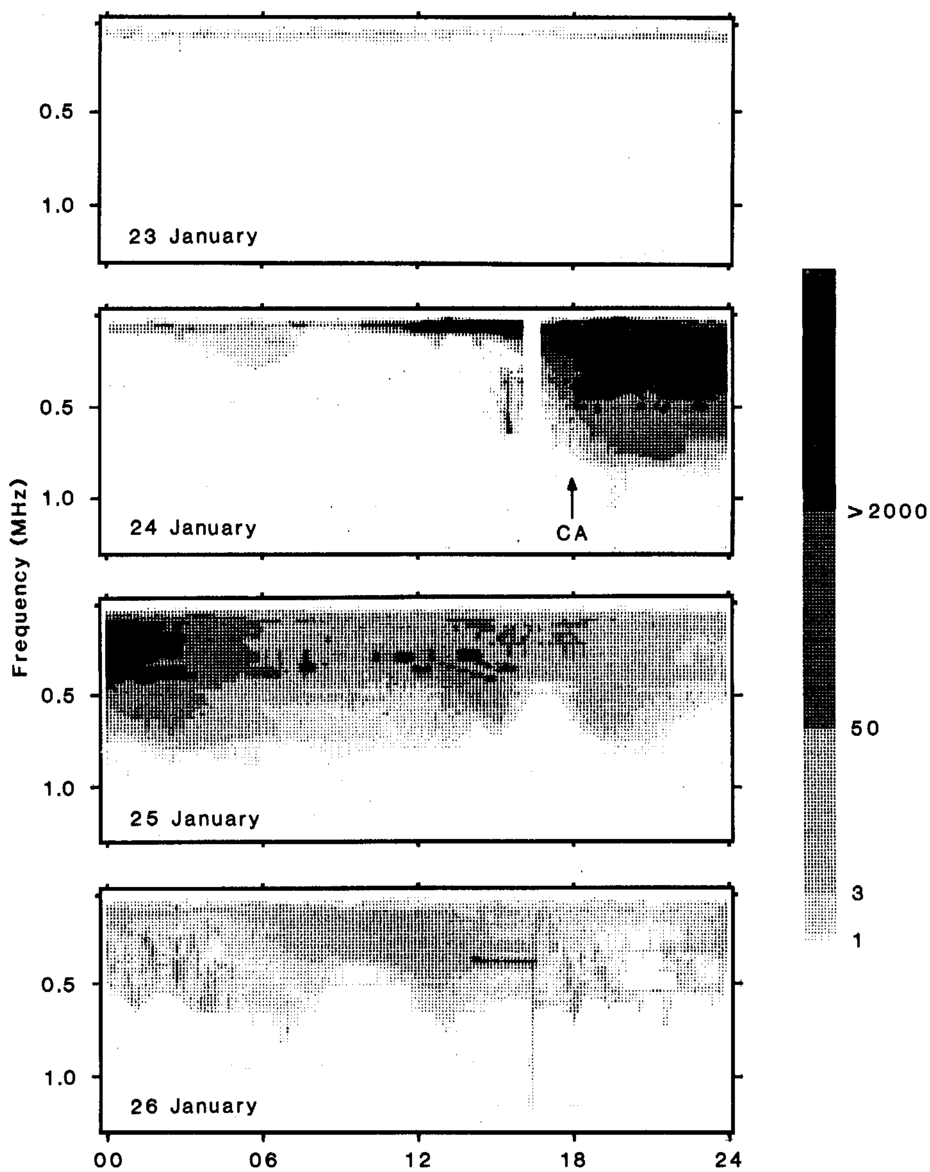

Fig. 2. Dynamic spectra in the frequency range 1.2 to 1326.0 kHz for the 4-day period near closest approach (CA). Increasing darkness corresponds to increasing intensity according to the indicated scale.

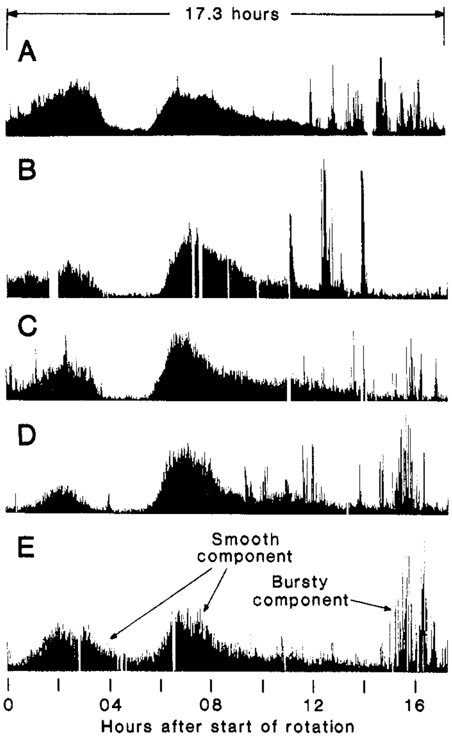

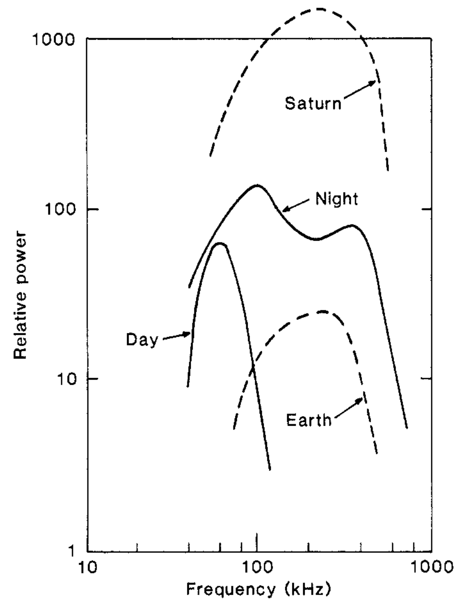

Fig. 3 (left). Five consecutive rotations at 481.2 kHz. The start time of each rotation (in spacecraft event time) is 1200 25 January (A), 0518 26 January (B), 2236 26 January (C), 1554 27 January (D), and 0912 28 January (E). Fig. 4 (right). The median observed spectrum for both the inbound (day) and outbound (night) portions of Voyager 2's trajectory; also shown for comparison are the corresponding median spectra for Earth and Saturn. A relative power of 1 corresponds to a flux density of 100 Jy at a distance of 1.0 astronomical unit.

however, that longitude alone defines a large part of the variation of the Uranus emission, perhaps because of the very large tilt of the dipole axis with respect to the rotation axis. Therefore we defer discussion of latitudinal variations.

On the outbound trajectory, when the radio emissions were at their strongest at frequencies below 300 kHz (or above 300 kHz in the middle of the bite), Voyager was viewing down into the negative tip of the Uranian dipole. At the same time the positive tip of the dipole lay at a large angular distance from the spacecraft, and emissions from it were blocked by the body of the planet. The radio waves, if they came from the negative tip (as is suggested by these angular relations), propagated in the opposite sense to the field direction in the source. The polarization of these waves was left-hand. This relation between polarization and propagation direction in the source defines the extraordinary mode of magnetoionic theory. For many planetary emissions from Earth, Jupiter, and Saturn, the emission mode is also the extraordinary mode.

If the source of the radio emissions on the inbound trajectory is also near the negative tip of the dipole, then on the lines of force that loop into the dayside magnetosphere the same relation between polarization and direction of propagation through the source magnetic field can hold. That only the negative tip is involved on the inbound trajectory is not as unambiguous as it was on the outbound trajectory, because the positive dipole tip has lines of force on the nightside of Uranus that also point away from Voyager and from which emission would not be completely blocked by the planet.

Examination of Fig. 6 shows that the 78.0- and 97.2-kHz radiations are generated at great elevations but close together in space. Nevertheless, Fig. 1 shows a critical distinction before closest approach: emission was weak at 97.2 kHz but strong at 78.0 kHz and lower. Yet 97.2-kHz emission was strong after closest approach, had the same general polarization as 78.0-kHz emissions both before and after closest approach, and peaked at the same general longitude as 78.0-kHz emissions both before and after closest approach. We conclude that 97.2-kHz emission must have been generated by Uranus before Voyager's closest approach, when there was little emission above 78.0 kHz. Before closest approach, then, the emissions at 97.2 kHz for the most part must not have reached the spacecraft. This distinction between 78.0- and 97.2-kHz emission is contrary to the usual distinction between low- and high-frequency waves: the lower frequency is expected to be refracted by a larger amount, or to be beamed more narrowly, whereas the higher frequency is expected to penetrate a given propagation barrier more easily. Furthermore, the cutoff frequency, near 95 kHz, represents a high-frequency cutoff; emissions at higher frequencies (up to as much as 800 kHz) did not reach the spacecraft before closest approach, even as emissions as low as 40 kHz appeared to reach it.

We suggest that a region of dense electron plasma then lay between the source of the 97.2-kHz emissions and the spacecraft. It must have been dense enough and at an altitude just high enough to block the 97.2-kHz emissions but not high enough to block the emissions with lower frequencies and higher sources. Thus the difference between 78.0- and 97.2-kHz emissions before closest approach defines the position in space of the boundary of a large cloud of plasma on the dayside of Uranus. This cloud apparently lay between L shells 3 and 4 and continued down toward the planet's surface with density increasing at least in proportion to the local electron cyclotron frequency. Without this continuous distribution down to the surface, we would see the high-frequency emissions characteristic of the outbound trajectory before as well as after closest approach. This high-altitude plasma cloud may exist only on the dayside.

In addition, the cutoff was exceedingly sharp in space. Blocking 97.2-kHz radiation requires a plasma of about 100 electrons per

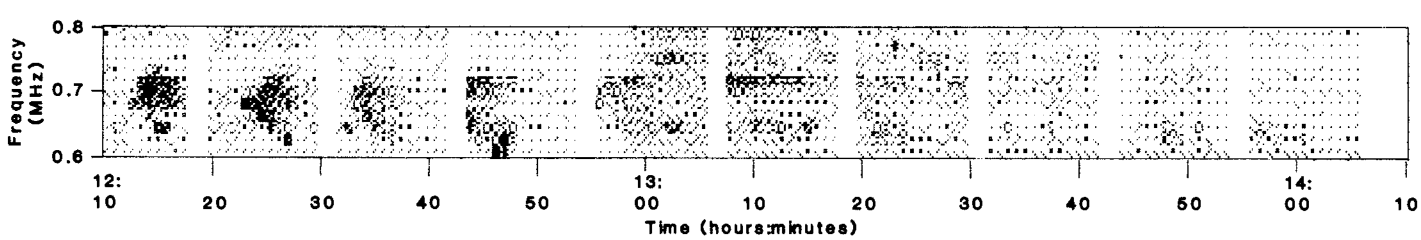

Fig. 5. Dynamic spectrum showing a sequence of periodic vertex-early arcs. The events continue from about 1120 until 1330 spacecraft event time, with a period of about 10 minutes.

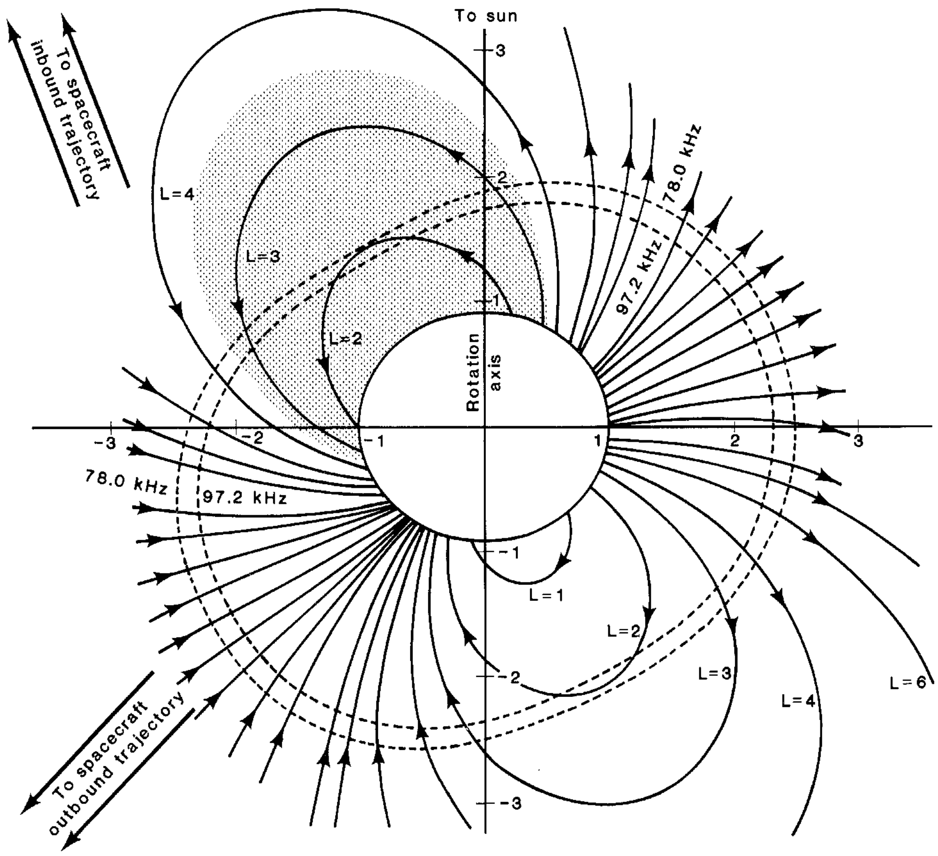

Fig. 6. The meridian plane containing the Uranian rotation axis (the vertical axis of the figure) and magnetic dipole. Dipole lines of force, with L-shell designations, and the inferred lobelike plasmasphere (stippled region) are shown.

cubic centimeter, but the radiation at both 78.0 and 58.8 kHz is generated close to the same point in space and yet escapes. A rough estimate of the plasma density gradient is possible. The height difference between the 78.0- and 97.2-kHz gyro emission surfaces is about 0.2 R_U in the region of interest. In one possible source region this radial height projects (on the plane perpendicular to the line of sight) to a much smaller value, perhaps about 0.05 R_U, over which the density declines to $(78/97)^2$ or 0.65 of its value at the position where the 97.2-kHz radiation was blocked. This decline, if it were to continue linearly, would produce a zero-density plasma within 0.15 R_U. Outside this L shell, the plasma density was so low that even 58.2-kHz radiation was scarcely affected. The corresponding plasma density is therefore much less than 42 electrons per cubic centimeter.

A sharply defined plasma cloud, called the plasmasphere, surrounds Earth (*5*). Earth's plasmapause is controlled by a dawn-to-dusk electric field across the magnetosphere and its tail. By analogy, we would expect that plasma outside the Uranian plasmasphere moves under control of convecting tubes of magnetic force. These tubes ultimately would interact with the magnetospheric boundary. The plasma inside the Uranian plasmasphere would be controlled by the planet's rotation. The crossover region from external to internal control would, according to this expectation, create the sharp plasmapause that we may have detected.

REFERENCES AND NOTES

1. J. W. Warwick, J. B. Pearce, R. G. Peltzer, A. C. Riddle, *Space Sci. Rev.* **21**, 309 (1977).
2. D. A. Gurnett and C. K. Goertz, *J. Geophys. Res.* **86**, 717 (1981).
3. J. W. Warwick *et al.*, *Science* **215**, 582 (1982).
4. N. F. Ness *et al.*, *ibid.* **233**, 85 (1986).
5. D. P. Stern and N. F. Ness, *Annu. Rev. Astron. Astrophys.* **20**, 139 (1982).

28 March 1986; accepted 5 May 1986

First Plasma Wave Observations at Uranus

D. A. Gurnett, W. S. Kurth, F. L. Scarf, R. L. Poynter

Radio emissions from Uranus were detected by the Voyager 2 plasma wave instrument about 5 days before closest approach at frequencies of 31.1 and 56.2 kilohertz. About 10 hours before closest approach the bow shock was identified by an abrupt broadband burst of electrostatic turbulence at a radial distance of 23.5 Uranus radii. Once Voyager was inside the magnetosphere, strong whistler-mode hiss and chorus emissions were observed at radial distances less than about 8 Uranus radii, in the same region where the energetic particle instruments detected intense fluxes of energetic electrons. Various other plasma waves were also observed in this same region. At the ring plane crossing, the plasma wave instrument detected a large number of impulsive events that are interpreted as impacts of micrometer-sized dust particles on the spacecraft. The maximum impact rate was about 30 to 50 impacts per second, and the north-south thickness of the impact region was about 4000 kilometers.

The Voyager 2 flyby of Uranus on 24 January 1986 revealed that the planet has a large and unusual magnetosphere. Here we present an overview of the principal results from the plasma wave (PWS) instrument (*1*), beginning with the first detection of radio emissions from Uranus and ending with results obtained a few days after closest approach.

Radio emissions. Because radio emissions escaping from the magnetosphere were expected to provide the first clear indication of a planetary magnetic field (*2*), the detection of radio bursts was an important objective as Voyager approached Uranus. In contrast to the situation at Jupiter and Saturn, radio emissions were not observed until the spacecraft was close to the planet. The first clear radio emissions from Uranus were detected by the PWS instrument on 19 January 1986, only about 5 days before closest approach, at frequencies of 31.1 and 56.2 kHz (Fig. 1). At this time Voyager was at a radial distance of about 275 Uranus radii (R_U). The emission is strongest in the 31.1-kHz channel and is highly variable, with numerous sporadic bursts on time scales of seconds

D. A. Gurnett and W. S. Kurth, Department of Physics and Astronomy, University of Iowa, Iowa City, IA 52242.
F. L. Scarf, TRW Space and Technology Group, Redondo Beach, CA 90278.
R. L. Poynter, Jet Propulsion Laboratory, California Institute of Technology, Pasadena, CA 91109.